Current control reference calculation issues for the operation of renewable source grid interface VSCs under unbalanced voltage sags

Adrià Junyent-Ferré, *Student Member, IEEE*, Oriol Gomis-Bellmunt, *Member, IEEE*,
Tim C. Green, *Senior Member, IEEE* and Diego E. Soto-Sanchez, *Member, IEEE*

Abstract

This paper analyzes the current reference calculation for the control of grid-connected voltage source converters meant to operate under voltage unbalanced sags produced by grid faults. The well known reference calculation method that allows to control the active power ripple produced by the existence of negative sequence components in the grid voltage is extensively analyzed. A type of voltage sag which produces unfeasible current reference values is identified and a possible workaround is proposed. Also, the need to compensate the power ripple produced by the filter inductance of the converter is demonstrated and a extension of the calculation method to compensate for this is introduced. The theoretical results are confirmed using simulation tools and experimental tests.

I. Introduction

Voltage source converters (VSCs) are used in a number of applications ranging from low voltage microgrid applications [1] to large VSC-HVDC power converters for offshore wind generation [2]. VSC has been successfully used as a grid connection interface for most renewable energy sources as doubly fed induction generator (DFIG) and permanent magnet synchronous generator (PMSG) wind turbines and photovoltaic panels. Synchronous reference frame vector control (SRFVC) is the most popular technique for the control of the VSC and has been demonstrated to provide good performance for balanced operation [3], [4].

The work of Adrià Junyent-Ferré and Oriol Gomis-Bellmunt was supported by the *Ministerio de Ciencia e Innovación* under the project ENE2009-08555.

A. Junyent Ferré and O. Gomis-Bellmunt are with the Centre d'Innovació Tecnològica en Convertidors Estàtics i Accionaments (CITCEA-UPC), Departament d'Enginyeria Elèctrica, Universitat Politècnica de Catalunya. ETS d'Enginyeria Industrial de Barcelona, Av. Diagonal, 647, Pl. 2. 08028 Barcelona, Spain. Tel: +34934016727, e-mail: adria.junyent@citcea.upc.edu. Oriol Gomis-Bellmunt is also with the Institute for Energy Research of Catalonia IREC.

T.C. Green and D.E. Soto-Sanchez are with the Department of Electronic and Electrical Engineering, Imperial college, London, SW7 2AZ, UK.

The increasing penetration of renewable energy in the grid, has brought a need to develop new methodologies of control for this devices to allow them to remain connected to the grid during different types of grid disturbances and avoid having to disconnect, a feature which is commonly known as ride-through.

Voltage sags are the most frequent type of grid disturbances. They are reductions of the voltage amplitude and are usually classified between balanced, when the reduction of the voltage is the same for each phase, and unbalanced otherwise. Balanced voltage sags are usually caused by the starting transients of large machines and three phase short circuits. Unbalanced voltage sags are caused by single phase or two phase short-circuits and are the most common type of sags [5].

The ride-through capability for balanced voltage sags have been addressed in the past and have been shown to be possible by introducing power reduction mechanisms to the SRFVC, as the reduction of the grid voltage causes the converter to reach its maximum allowed current which in turn causes the voltage of the DC bus to rise due to the excess power input to the bus [6], [7].

On the other hand, ride-through capabilities for unbalanced voltage sags present a number of challenges. The presence of negative sequence components in the voltage causes a ripple in the power injected to the AC grid. This causes the DC bus voltage to have a ripple, which in some cases may be critical. Also, the existence of negative sequence voltage causes negative sequence current to appear which needs to be controlled to reduce the ripple of the DC bus. Conventional SRFVC is designed to control positive sequence currents and it exhibits poor performance when controlling negative sequence.

Different choices for alternative designs of the current controllers have been suggested in the past. In [8] a current reference calculation scheme was proposed that enables suppressing the active power oscillations during unbalanced voltage sags using conventional SRFVC with enhanced current controllers able to track a reference current signals containing both positive and negative sequence. In [9] a different current control design with a double SRFVC and independent controllers for positive and negative components was introduced. In [10] and [11] this current control is used for a coordinated control of the back-to-back converter of a DFIG turbine to enable the suppression of the machine torque and the ripple of the DC bus voltage caused by the network unbalances. In [12] a double SRFVC using linear quadratic regulators (LQR) current controllers is proposed for the operation of a PMSG wind turbine under unbalanced voltage sags. In [13] and [14], coordinated control of the back-to-back converter of the DFIG using stationary frame current control with proportional-resonant controllers is proposed. Stationary frame control has also been proved to provide good performance under unbalance operation of VSC while simplifying the structure of the current controller [15].

The previously mentioned works use current reference calculation methods deriving from the one introduced in [8] that uses negative sequence current to compensate for the oscillation of the power due to the presence of negative sequence in the grid voltage. The present paper analyzes this method and provides a critic analysis and some remarks on its limitations and some important weak points which to the best of the knowledge of the authors have not been addressed in the past. Also, modifications of the method to solve for this problems are proposed.

The paper is organized as follows: the equations needed to model the AC side of the VSC inverter are obtained

in Section II, these equations are then used in Section III to analyze the steady state for balanced operation and to obtain the current reference calculation equations of the conventional vector control. In Section IV the steady state equations for unbalanced operation are obtained and the current reference calculation formulas to control the power output of the converter are derived and discussed. Finally the conclusions drawn in the previous section are tested on a simulation model in Section V and on an experimental platform in Section VI.

II. Modeling of the grid-connected VSC

The basic scheme of a grid-connected VSC is presented in Figure 1, the purpose of the VSC is to connect a DC bus which is fed with the power from a renewable generator to the AC grid through a switching device. As the voltage of the DC bus is desired to be constant and the AC grid usually has a low impedance, a filtering inductor is used to connect the switching device to the grid.

The equations that relate the voltage on both sides of the inductor and the current flowing throw it can be written as [4]:

$$v_{ln}^{abc} + (v_{nl} - v_{nz}) \begin{bmatrix} 1 & 1 & 1 \end{bmatrix}^T = r_l i_l^{abc} + L_l \frac{d}{dt} i_l^{abc} + v_{zn}^{abc} \tag{1}$$

and

$$i_{la} + i_{lb} + i_{lc} = 0 \tag{2}$$

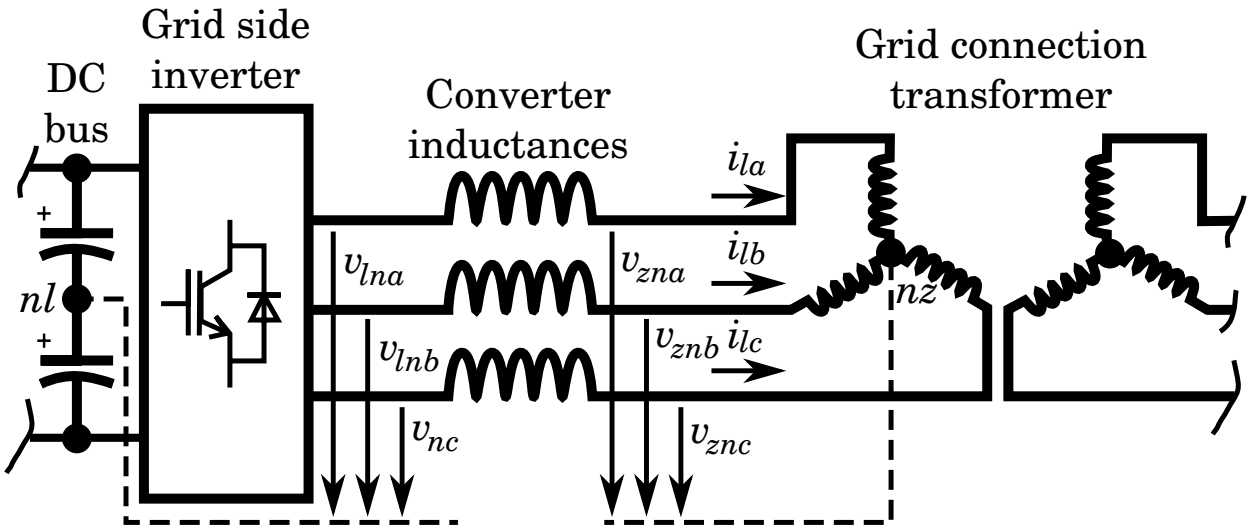

Fig. 1. Grid connected VSC inverter.

By combining these equations, the following relation between the voltage of both neutrals is obtained:

$$v_{nl} - v_{nz} = \frac{1}{3} \left(v_{zna} + v_{znb} + v_{znc} - v_{lna} - v_{lnb} - v_{lnc} \right) \tag{3}$$

Using this, the voltage equation in (1) can be rewritten in a more compact form as:

$$v_l^{abc} = r_l i_l^{abc} + L_l \frac{d}{dt} i_l^{abc} + v_z^{abc} \tag{4}$$

by defining v_l^{abc} and v_z^{abc} as:

$$\begin{cases} v_l^{abc} \triangleq v_{ln}^{abc} - (v_{lna} + v_{lnb} + v_{lnc}) \begin{bmatrix} 1 & 1 & 1 \end{bmatrix}^T \\ v_z^{abc} \triangleq v_{zn}^{abc} - (v_{zna} + v_{znb} + v_{znc}) \begin{bmatrix} 1 & 1 & 1 \end{bmatrix}^T \end{cases} \tag{5}$$

Note that (2) assumes that:

$$\begin{cases} v_{la} + v_{lb} + v_{lc} = 0 \\ v_{za} + v_{zb} + v_{zc} = 0 \end{cases} \tag{6}$$

To obtain the steady state equations, it is useful to introduce a the so called Park variable change matrix. This matrix, for a given θ Park reference angle, is defined as [16]:

$$T(\theta) = \frac{2}{3} \begin{bmatrix} \cos(\theta) & \cos(\theta - \frac{2\pi}{3}) & \cos(\theta + \frac{2\pi}{3}) \\ \sin(\theta) & \sin(\theta - \frac{2\pi}{3}) & \sin(\theta + \frac{2\pi}{3}) \\ \frac{1}{2} & \frac{1}{2} & \frac{1}{2} \end{bmatrix} \tag{7}$$

The $qd0$ reference frame representation $x^{abc}(t)$ of a generic $x^{abc}(t)$ signal in the Park reference frame with θ angle is defined as:

$$x^{qd0} \triangleq T(\theta) x^{abc} \tag{8}$$

Introducing the variable change to the system equation (4), it can be rewritten as a function of the new variables:

$$v_l^{qd} = \begin{bmatrix} r_l & L_l\dot{\theta} \\ -L_l\dot{\theta} & r_l \end{bmatrix} i_l^{qd} + L_l \frac{d}{dt} i_l^{qd} + v_z^{qd} \tag{9}$$

Note that the use of the Park reference frame allows to suppress the 0 component equation, which is redundant as $i_{l0} \equiv 0$ according to (2).

III. Analysis of the current reference calculation for balanced operation

According to [17], a generic $x^{abc}(t)$ three phase positive sequence signal is a function of time that can be described as:

$$x^{abc}(t) = \sqrt{2} X \begin{bmatrix} \cos(\omega_e t + \varphi_x) \\ \cos(\omega_e t + \varphi_x - \frac{2\pi}{3}) \\ \cos(\omega_e t + \varphi_x + \frac{2\pi}{3}) \end{bmatrix} \tag{10}$$

By choosing the $\frac{d}{dt}\theta = \omega_e$ for the Park reference angle, the transformed signal becomes a vector of constants:

$$x^{qd0}(t) = T(\omega_e t + \varphi) x^{abc} = \sqrt{2} X \begin{bmatrix} \cos(\varphi_x - \varphi) \\ -\sin(\varphi_x - \varphi) \\ 0 \end{bmatrix} \tag{11}$$

We define:

$$\begin{bmatrix} x_q^{ss} \\ x_d^{ss} \end{bmatrix} \triangleq \begin{bmatrix} \sqrt{2} X \cos(\varphi_x - \varphi) \\ -\sqrt{2} X \sin(\varphi_x - \varphi) \end{bmatrix} \tag{12}$$

Considering a balanced case where both the inverter voltage v_l^{abc} and the grid voltage v_z^{abc} are positive sequence signals, choosing θ to match the angle of v_{za} and assuming the derivatives of the current to become zero in steady state, the following relations can be obtained from (9):

$$\begin{cases} v_{lq}^{ss} - v_{zq}^{ss} = r_l i_{lq}^{ss} + L_l \omega_e i_{ld}^{ss} \\ v_{ld}^{ss} = r_l i_{ld}^{ss} - L_l \omega_e i_{lq}^{ss} \end{cases} \tag{13}$$

These equations can be used to solve for the current needed to have a certain steady state power. According to [18], active and reactive power can be calculated using the voltage and current in the qd form as:

$$\begin{cases} P &= \frac{3}{2}\left(v_q i_q + v_d i_d\right) = \frac{3}{2}\{v^{qd}\}^T \begin{bmatrix} 1 & 0 \\ 0 & 1 \end{bmatrix} i^{qd} \\ Q &= \frac{3}{2}\left(v_q i_d - v_d i_q\right) = \frac{3}{2}\{v^{qd}\}^T \begin{bmatrix} 0 & 1 \\ -1 & 0 \end{bmatrix} i^{qd} \end{cases} \tag{14}$$

Substituting for the grid connection point:

$$\begin{cases} P_z &= \frac{3}{2} v_{zq} i_{lq} \\ Q_z &= \frac{3}{2} v_{zq} i_{ld} \end{cases} \tag{15}$$

Assuming v_{zd} to be zero, which can be ensured by an adequate tracking of the grid voltage measure using a phase locked loop (PLL), (15) implies that active and reactive power are proportional to the i_{lq} and i_{ld} respectively. This is commonly used to calculate a current reference value for the current control from a power reference signal usually generated by the DC bus voltage regulator and a reactive power command:

$$\begin{cases} i_{lq}^* = \frac{2}{3}\frac{P_z^*}{v_{zq}} \\ i_{ld}^* = \frac{2}{3}\frac{Q_z^*}{v_{zq}} \end{cases} \tag{16}$$

One drawback of this reference calculation method is that it ignores the power loss due to the resistance of the converter filter and its dynamic behavior. Thus even having a perfect current control, the active power output of the converter P_l will not be equal to the power on the grid connection point P_z and the DC bus voltage regulator will need to be able to compensate for that difference. Usually this is not a important issue as the filter resistance is small and the regulators used to control the DC bus are designed for disturbance rejection. On the other hand, one possible workaround to match the DC bus voltage regulator power command to the actual power output by the inverter in steady state is to subtract the losses due to the filter to the active power reference value:

$$P_z^* = P_l^* - r_l\left(\left(i_{lq}^*\right)^2 + \left(i_{ld}^*\right)^2\right) \tag{17}$$

Note that i_{lq}^* and i_{ld}^* depend on the choice of P_z^*. As the losses due to filter resistance will be very small in comparison with P_l^*, the actual solution may be close to the initial guess P_l^*, thus one possible approach is to iteratively solve for the current as:

$$\begin{cases} \left(i_{lq}^*\right)_{n+1} = \frac{2}{3}\frac{\left(P_z^*\right)_n}{v_{zq}} \\ \left(i_{ld}^*\right)_{n+1} = \frac{2}{3}\frac{\left(Q_z^*\right)_n}{v_{zq}} \end{cases} \tag{18}$$

with

$$\left(P_z^*\right)_n = P_l^* - r_l\left(\left(i_{lq}^*\right)_n^2 + \left(i_{ld}^*\right)_n^2\right) \tag{19}$$

IV. Analysis of the current reference calculation for unbalanced operation

According to [17] a three phase signal with positive and negative sequence components can be described as:

$$x^{abc}(t) = x_+^{abc}(t) + x_-^{abc}(t) \tag{20}$$

where

$$x_+^{abc}(t) = \sqrt{2}X^+ \begin{bmatrix} \cos(\omega_e t + \varphi_x^+) \\ \cos(\omega_e t + \varphi_x^+ - \frac{2\pi}{3}) \\ \cos(\omega_e t + \varphi_x^+ + \frac{2\pi}{3}) \end{bmatrix} \tag{21}$$

$$x_-^{abc}(t) = \sqrt{2}X^- \begin{bmatrix} \cos(\omega_e t + \varphi_x^-) \\ \cos(\omega_e t + \varphi_x^- + \frac{2\pi}{3}) \\ \cos(\omega_e t + \varphi_x^- - \frac{2\pi}{3}) \end{bmatrix} \tag{22}$$

Unlike in the balanced case, here it is not possible to transform the time varying signal $x^{abc}(t)$ into a constant signal by using the Park variable change matrix. On the other hand it is possible to decompose the system in two decoupled systems corresponding to the positive and the negative sequence which can be analyzed using the same procedure as in the balanced case due to the linear properties of the dynamics of the system and the symmetrical nature of its impedances [17].

The positive sequence magnitudes can be transformed into constant signals by choosing a Park reference angle matching the angle of the a phase of the original signal:

$$x_+^{qd}(t) = T(\omega_e t + \varphi^+) x_+^{abc}(t) = \sqrt{2}X^+ \begin{bmatrix} \cos(\varphi_x^+ - \varphi^+) \\ -\sin(\varphi_x^+ - \varphi^+) \end{bmatrix} \tag{23}$$

while the negative sequence magnitudes can be transformed into constants by choosing θ to be equal to the angle of the a phase multiplied by -1:

$$x_-^{qd}(t) = T(-\omega_e t - \varphi^-) x_-^{abc}(t) = \sqrt{2}X^- \begin{bmatrix} \cos(\varphi_x^- - \varphi^-) \\ \sin(\varphi_x^- - \varphi^-) \end{bmatrix} \tag{24}$$

As in the balanced case we define the steady state components in the synchronous reference frame as:

$$\begin{bmatrix} x_q^+ \\ x_d^+ \end{bmatrix} \triangleq \begin{bmatrix} \sqrt{2}X^+ \cos(\varphi_x^+ - \varphi^+) \\ -\sqrt{2}X^+ \sin(\varphi_x^+ - \varphi^+) \end{bmatrix} \tag{25}$$

and

$$\begin{bmatrix} x_q^- \\ x_d^- \end{bmatrix} \triangleq \begin{bmatrix} \sqrt{2}X^- \cos(\varphi_x^- - \varphi^-) \\ \sqrt{2}X^- \sin(\varphi_x^- - \varphi^-) \end{bmatrix} \tag{26}$$

Also, as in the balanced case, the steady state equations can be obtained from (9) by assuming the derivatives of the current to be zero:

$$\begin{cases} v_{lq}^+ - v_{zq}^+ = r_l i_{lq}^+ + L_l \omega_e i_{ld}^+ \\ v_{ld}^+ = r_l i_{ld}^+ - L_l \omega_e i_{lq}^+ \end{cases} \tag{27}$$

and

$$\begin{cases} v_{lq}^{-} - v_{zq}^{-} = r_l i_{lq}^{-} - L_l \omega_e i_{ld}^{-} \\ v_{ld}^{-} = r_l i_{ld}^{-} + L_l \omega_e i_{lq}^{-} \end{cases} \tag{28}$$

As of the power equations (14), they include multiplications between voltage and current, thus they are not linear and it is no longer possible to separate positive and negative sequence, as there will be crossed products of terms from both. To calculate the power, the steady state positive and negative sequence magnitudes are transformed to a common reference frame with $\theta = 0$ as:

$$P = \frac{3}{2}\{R(-\omega_e t - \varphi^{+})v_{+}^{qd} + R(\omega_e t + \varphi^{-})v_{-}^{qd}\}^{T} \cdot \begin{bmatrix} 1 & 0 \\ 0 & 1 \end{bmatrix} \left(R(-\omega_e t - \varphi^{+})i_{+}^{qd} + R(\omega_e t + \varphi^{-})i_{-}^{qd}\right) \tag{29}$$

and

$$Q = \frac{3}{2}\{R(-\omega_e t - \varphi^{+})v_{+}^{qd} + R(\omega_e t + \varphi^{-})v_{-}^{qd}\}^{T} \cdot \begin{bmatrix} 0 & 1 \\ -1 & 0 \end{bmatrix} \left(R(-\omega_e t - \varphi^{+})i_{+}^{qd} + R(\omega_e t + \varphi^{-})i_{-}^{qd}\right) \tag{30}$$

where $R(\theta)$ is a rotation matrix defined as:

$$R(\theta) = \begin{bmatrix} \cos(\theta) & -\sin(\theta) \sin(\theta) & \cos(\theta) \end{bmatrix} \tag{31}$$

Note that it can easily be proven that the following relation exists between $T(\theta)$ and $R(\theta)$:

$$T(\theta) \equiv \begin{bmatrix} R(\theta) & 0 \\ 0 & 1 \end{bmatrix} T(0) \tag{32}$$

The resulting equation of the active power can be written as:

$$P = P_0 + P_{\cos}\cos(2\omega_e t + \varphi^{+} + \varphi^{-}) + P_{\sin}\sin(2\omega_e t + \varphi^{+} + \varphi^{-}) \tag{33}$$

where

$$\begin{cases} P_0 = \frac{3}{2}\left(v_q^{+} i_q^{+} + v_d^{+} i_d^{+} + v_q^{-} i_q^{-} + v_d^{-} i_d^{-}\right) \\ P_{\cos} = \frac{3}{2}\left(v_q^{+} i_q^{-} + v_d^{+} i_d^{-} + v_q^{-} i_q^{+} + v_d^{-} i_d^{+}\right) \\ P_{\sin} = \frac{3}{2}\left(-v_q^{+} i_d^{-} + v_d^{+} i_q^{-} + v_q^{-} i_d^{+} - v_d^{-} i_q^{+}\right) \end{cases} \tag{34}$$

The reactive power expression can be written as:

$$Q = Q_0 + Q_{\cos}\cos(2\omega_e t + \varphi^{+} + \varphi^{-}) + Q_{\sin}\sin(2\omega_e t + \varphi^{+} + \varphi^{-}) \tag{35}$$

where

$$\begin{cases} Q_0 = \frac{3}{2}\left(v_q^{+} i_d^{+} - v_d^{+} i_d^{+} + v_q^{-} i_d^{+} - v_d^{-} i_d^{-}\right) \\ Q_{\cos} = \frac{3}{2}\left(v_q^{+} i_d^{-} - v_d^{+} i_q^{-} + v_q^{-} i_d^{+} - v_d^{-} i_q^{+}\right) \\ Q_{\sin} = \frac{3}{2}\left(v_q^{+} i_q^{-} + v_d^{+} i_d^{-} - v_q^{-} i_q^{-} - v_d^{-} i_d^{+}\right) \end{cases} \tag{36}$$

Unlike the balanced case, the steady state active and reactive power contains a constant component plus time-varying sine components with a frequency of twice the grid frequency. Also, although six power magnitudes were defined, there only exist four independent currents. Thus it is only possible to decide the value of four of the six power terms while the rest depend on the choice of the previous ones. In this situation it is common to choose to

constraint the value of the three components of the active power, which have a direct effect in the evolution of the DC bus voltage, and the mean value of the reactive power. Usually the reference value for the sine components of the active power is set to be zero to avoid the ripple in the DC bus voltage. However, it can also be set to match another time-varying power input as described in [11]. The equations to solve for the power on the grid connection point of the converter are:

$$\begin{cases} P_{z0} & = \frac{3}{2}\left(v_{zq}^{+}i_{lq}^{+} + v_{zq}^{-}i_{lq}^{-}\right) \\ P_{z\cos} & = \frac{3}{2}\left(v_{zq}^{+}i_{lq}^{-} + v_{zq}^{-}i_{lq}^{+}\right) \\ P_{z\sin} & = \frac{3}{2}\left(-v_{zq}^{+}i_{ld}^{-} + v_{zq}^{-}i_{ld}^{+}\right) \\ Q_{z0} & = \frac{3}{2}\left(v_{zq}^{+}i_{ld}^{+} + v_{zq}^{-}i_{ld}^{-}\right) \end{cases} \tag{37}$$

Solving to obtain the reference current for a given active and reactive power reference, the following relation is obtained:

$$\begin{cases} i_{lq}^{+} = \frac{2}{3}\left(\frac{v_{zq}^{+}}{\left(v_{zq}^{+}\right)^2-\left(v_{zq}^{-}\right)^2}P_{z0}^{*} - \frac{v_{zq}^{-}}{\left(v_{zq}^{+}\right)^2-\left(v_{zq}^{-}\right)^2}P_{z\cos}\right) \\ i_{ld}^{+} = \frac{2}{3}\left(\frac{v_{zq}^{+}}{\left(v_{zq}^{+}\right)^2+\left(v_{zq}^{-}\right)^2}Q_{z0}^{*} + \frac{v_{zq}^{-}}{\left(v_{zq}^{+}\right)^2+\left(v_{zq}^{-}\right)^2}P_{z\sin}\right) \\ i_{lq}^{-} = \frac{2}{3}\left(-\frac{v_{zq}^{-}}{\left(v_{zq}^{+}\right)^2-\left(v_{zq}^{-}\right)^2}P_{z0}^{*} + \frac{v_{zq}^{+}}{\left(v_{zq}^{+}\right)^2-\left(v_{zq}^{-}\right)^2}P_{z\cos}\right) \\ i_{ld}^{-} = \frac{2}{3}\left(\frac{v_{zq}^{-}}{\left(v_{zq}^{+}\right)^2+\left(v_{zq}^{-}\right)^2}Q_{z0}^{*} - \frac{v_{zq}^{+}}{\left(v_{zq}^{+}\right)^2+\left(v_{zq}^{-}\right)^2}P_{z\sin}\right) \end{cases} \tag{38}$$

As in the balanced case, this calculation neglects the difference between the active power in the grid connection point of the converter and the actual active power output of the inverter. The active power on the inverter terminals can be written as a function of the active power output to the grid as:

$$P_{l0} = P_{z0} + r_l\left(\left(i_{lq}^{+}\right)^2 + \left(i_{ld}^{+}\right)^2 + \left(i_{lq}^{-}\right)^2 + \left(i_{ld}^{-}\right)^2\right) \tag{39}$$

$$P_{l\cos} = P_{z\cos} + 3r_l\left(i_{lq}^{+}i_{lq}^{-} + i_{ld}^{+}i_{ld}^{-}\right) + 3\omega_e L_l\left(-i_{lq}^{+}i_{ld}^{-} + i_{ld}^{+}i_{lq}^{-}\right) \tag{40}$$

$$P_{l\sin} = P_{z\sin} - 3r_l\left(i_{lq}^{+}i_{ld}^{-} - i_{ld}^{+}i_{lq}^{-}\right) - 3\omega_e L_l\left(i_{lq}^{+}i_{lq}^{-} + i_{ld}^{+}i_{ld}^{-}\right) \tag{41}$$

Note that unlike the balanced case, the voltage drop in the inductor not only affects the mean value of the active power, which can be properly compensated by the DC bus voltage controller, but also affects the time-varying terms of the active power, which sometimes are controlled in a open loop way by setting them to be zero.

As it was suggested in the balanced case, one workaround for this problem is to iteratively solve for the current reference by correcting the active power reference value:

$$\left(i_{lq}^{+}\right)_{n+1} = \frac{2}{3}\frac{v_{zq}^{+}}{\left(v_{zq}^{+}\right)^2 - \left(v_{zq}^{-}\right)^2}\left(P_{z0}^{*}\right)_n - \frac{2}{3}\frac{v_{zq}^{-}}{\left(v_{zq}^{+}\right)^2 - \left(v_{zq}^{-}\right)^2}\left(P_{z\cos}^{*}\right)_n \tag{42}$$

$$\left(i_{ld}^{+}\right)_{n+1} = \frac{2}{3}\frac{v_{zq}^{+}}{\left(v_{zq}^{+}\right)^2+\left(v_{zq}^{-}\right)^2}Q_{z0}^{*} + \frac{2}{3}\frac{v_{zq}^{-}}{\left(v_{zq}^{+}\right)^2+\left(v_{zq}^{-}\right)^2}\left(P_{z\sin}^{*}\right)_n \quad (43)$$

$$\left(i_{lq}^{-}\right)_{n+1} = -\frac{2}{3}\frac{v_{zq}^{-}}{\left(v_{zq}^{+}\right)^2-\left(v_{zq}^{-}\right)^2}\left(P_{z0}^{*}\right)_n + \frac{2}{3}\frac{v_{zq}^{+}}{\left(v_{zq}^{+}\right)^2-\left(v_{zq}^{-}\right)^2}\left(P_{z\cos}^{*}\right)_n \quad (44)$$

$$\left(i_{ld}^{-}\right)_{n+1} = \frac{2}{3}\frac{v_{zq}^{-}}{\left(v_{zq}^{+}\right)^2+\left(v_{zq}^{-}\right)^2}Q_{z0}^{*} - \frac{2}{3}\frac{v_{zq}^{+}}{\left(v_{zq}^{+}\right)^2+\left(v_{zq}^{-}\right)^2}\left(P_{z\sin}^{*}\right)_n \quad (45)$$

where

$$\left(P_{z0}^{*}\right)_n = P_{l0}^{*} - r_l\left(\left(i_{lq}^{+}\right)_n^2+\left(i_{ld}^{+}\right)_n^2+\left(i_{lq}^{-}\right)_n^2+\left(i_{ld}^{-}\right)_n^2\right) \quad (46)$$

$$\left(P_{z\cos}^{*}\right)_n = P_{l\cos}^{*} - 3r_l\left(\left(i_{lq}^{+}\right)_n\left(i_{lq}^{-}\right)_n+\left(i_{ld}^{+}\right)_n\left(i_{ld}^{-}\right)_n\right) - 3\omega_e L_l\left(-\left(i_{lq}^{+}\right)_n\left(i_{ld}^{-}\right)_n+\left(i_{ld}^{+}\right)_n\left(i_{lq}^{-}\right)_n\right) \quad (47)$$

$$\left(P_{z\sin}^{*}\right)_n = P_{l\sin}^{*} + 3r_l\left(\left(i_{lq}^{+}\right)_n\left(i_{ld}^{-}\right)_n-\left(i_{ld}^{+}\right)_n\left(i_{lq}^{-}\right)_n\right) + 3\omega_e L_l\left(\left(i_{lq}^{+}\right)_n\left(i_{lq}^{-}\right)_n+\left(i_{ld}^{+}\right)_n\left(i_{ld}^{-}\right)_n\right) \quad (48)$$

Finally, one important result from (38), whose implications have not been addressed in previous works is that there exists a discontinuity that causes the reference current to become infinite when $v_{zq}^{+} = v_{zq}^{-}$ i.e. when the magnitude of the positive sequence of the voltage is equal to that of the negative sequence (there is no dominant voltage component). To analyze this particular situation, this condition is introduced in the equation of a unbalanced three phase signal (22) yelding:

$$v_z^{abc}(t) = 2A\begin{bmatrix}\cos(\frac{\varphi^+-\varphi^-}{2})\cos(\omega_e t+\frac{\varphi^++\varphi^-}{2})\\ \cos(\frac{\varphi^+-\varphi^-}{2}-\frac{2\pi}{3})\cos(\omega_e t+\frac{\varphi^++\varphi^-}{2})\\ \cos(\frac{\varphi^+-\varphi^-}{2}+\frac{2\pi}{3})\cos(\omega_e t+\frac{\varphi^++\varphi^-}{2})\end{bmatrix} \quad (49)$$

where $A \triangleq \sqrt{2}V_z^{+} = \sqrt{2}V_z^{-}$.

From this equation it can be seen that under such condition, each phase of v_z^{abc} become zero at the same time and it is not possible to get a constant power output from the converter without the need of an infinite current.

One possible solution to this problem would be to limit the result of (38) to a certain value by modulus. One important drawback of this solution is that in that case, it is not possible to assure that the resulting current reference will lead to the desired mean value of the active power, which is critical to maintain the desired mean value of the DC bus voltage.

A different approach based on combining two different reference calculation formulas is possible. The reference calculation expression (38) can be rewritten as:

$$\begin{cases} i_{lq}^{+} = \frac{2}{3}\frac{1}{v_{zq}^{+}}\left(P_{z0}^{*} + \alpha\frac{\left(\frac{v_{zq}^{-}}{v_{zq}^{+}}\right)^{2}P_{z0}^{*} - \frac{v_{zq}^{-}}{v_{zq}^{+}}P_{z\cos}^{*}}{1-\left(\frac{v_{zq}^{-}}{v_{zq}^{+}}\right)^{2}}\right) \\ i_{ld}^{+} = \frac{2}{3}\frac{1}{v_{zq}^{+}}\left(Q_{z0}^{*} + \alpha\frac{-\left(\frac{v_{zq}^{-}}{v_{zq}^{+}}\right)^{2}Q_{z0}^{*} + \frac{v_{zq}^{-}}{v_{zq}^{+}}P_{z\sin}^{*}}{1+\left(\frac{v_{zq}^{-}}{v_{zq}^{+}}\right)^{2}}\right) \\ i_{lq}^{-} = \frac{2}{3}\frac{\alpha}{v_{zq}^{+}}\left(P_{z\cos}^{*} + \frac{\left(\frac{v_{zq}^{-}}{v_{zq}^{+}}\right)^{2}P_{z\cos}^{*} - \frac{v_{zq}^{-}}{v_{zq}^{+}}P_{z0}^{*}}{1-\left(\frac{v_{zq}^{-}}{v_{zq}^{+}}\right)^{2}}\right) \\ i_{ld}^{-} = \frac{2}{3}\frac{\alpha}{v_{zq}^{+}}\left(-P_{z\sin}^{*} + \frac{\left(\frac{v_{zq}^{-}}{v_{zq}^{+}}\right)^{2}P_{z\sin}^{*} + \frac{v_{zq}^{-}}{v_{zq}^{+}}Q_{z0}^{*}}{1+\left(\frac{v_{zq}^{+}}{v_{zq}^{-}}\right)^{2}}\right) \end{cases} \tag{50}$$

where α is a parameter that allows switching between two different reference calculation methods. For $\alpha = 1$, (50) becomes equivalent to (38) whereas for $\alpha = 0$ the reference calculation formula becomes:

$$\begin{cases} i_{lq}^{+} = \frac{2}{3}\frac{1}{v_{zq}^{+}}P_{z0}* \\ i_{ld}^{+} = \frac{2}{3}\frac{1}{v_{zq}^{+}}Q_{z0}* \\ i_{lq}^{-} = 0 \\ i_{ld}^{-} = 0 \end{cases} \tag{51}$$

This equation is equivalent to the one used for the conventional vector control meant for balanced operation, thus the references for the negative sequence current are zero. From (37) it can be seen that this produces the desired mean value for the active and the reactive power but does not allow to control the sine time-varying terms of the active power.

One important remark that can be made by comparing (51) and (38) is that in general in the case of existence of negative sequence voltages in the grid, the suppression of the active power oscillation by injecting negative current leads to a reduction of the mean value of the active power. This in turn leads to the need of a higher positive sequence current to maintain the mean value of the active power. Thus, in case of a voltage sag, where usually the maximum allowed current becomes an issue, (38) is more likely to have problem to extract the needed active power to maintain the desired DC bus voltage. On the other hand, as the effect of the power oscillation on the DC bus voltage is directly related to the capacitance of the DC-side capacitor filter, this suggests that systems which use a DC-side capacitor filter with a small value of capacitance, which may be the standard practice in HVDC link systems, it may be necessary to overrate the current capability of the inverter to be able to compensate for the oscillations in case of a network unbalance.

V. Simulation testing of the proposed reference calculation scheme

In order to test the performance of the proposed control methods, a simulation of the response of the system to an unbalanced voltage sag is performed. The characteristic parameters of the simulated converter and the operation point for the simulation can be found in Table I. The rating of the converter and its switching frequency the same

as the grid-side inverter of the rotor converter of the 1 MW DFIG wind turbine in [19]. The machine-side inverter has been modeled as a constant power input of 300 kW with no ripple. Thus the power references for P_{lsin} and P_{lcos} will be set to zero to avoid a ripple in the DC bus voltage.

TABLE I
CHARACTERISTIC PARAMETERS OF THE SIMULATED SCENARIO.

Parameter	Units	Value	Description
V_z^N	690	V	Grid nominal voltage
P_l^N	300	kW	Nominal active power
Q_z^N	100	kVAr	Nominal reactive power
V_{DC}^N	1338	V	DC bus nominal voltage
r_l	0.05	Ω	Grid connection filter resistance
L_l	27	mH	Grid connection filter inductance
f_s	3	kHz	Inverter switching frequency
T_i	50	ms	Current control settling time
T_{PLL}	20	ms	Grid voltage PLL settling time

The response of the system to a unbalanced voltage sag is simulated using three different calculation methods (see Figure 2). The first one, referred as I, uses the formula presented in (50) for $\alpha = 0$, the second one, referred as II, uses the presented formula in (50) for $\alpha = 1$ plus the iterative compensation of the filter impedance and the third one, referred as III, uses the same formula as II but without compensating the filter impedance.

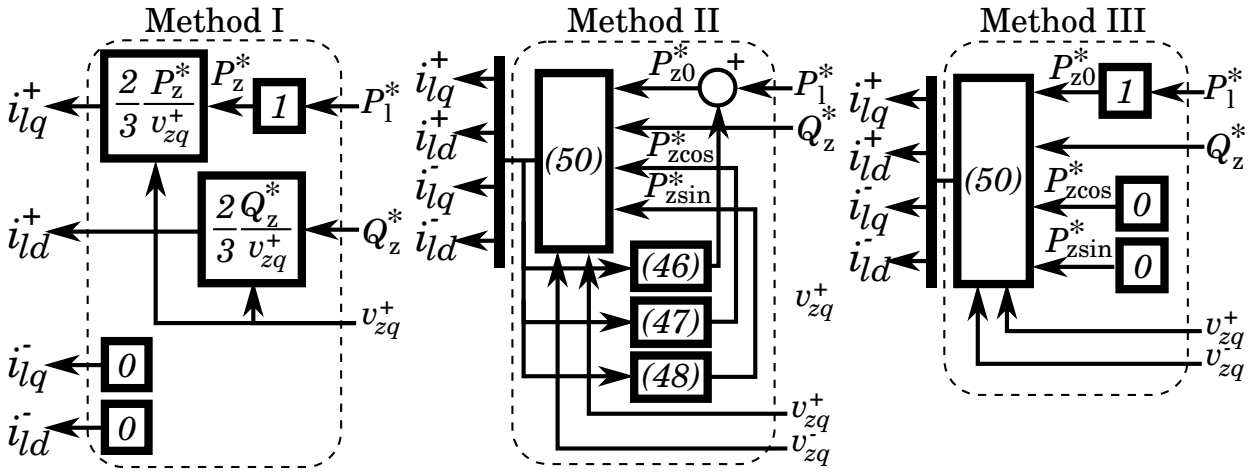

Fig. 2. Current reference calculation methods.

The simulated voltage sag corresponds to a two phase to ground sag which causes the voltage of two of the phases to drop by a 65%. The waveform of the grid voltage seen by the inverter is shown in Figure 3 and the

amplitude of the positive and negative sequence as measured by the phase locked loop (PLL) used by the controller is shown in Figure 4. Note this sag causes the positive sequence of the voltage to reduce to 0.36 pu and the negative sequence to appear with an amplitude of 0.30 pu, thus the ratio between the positive and the negative sequence amplitudes is 1.2 which is close to 1.0 which is the limit of the II and III methods.

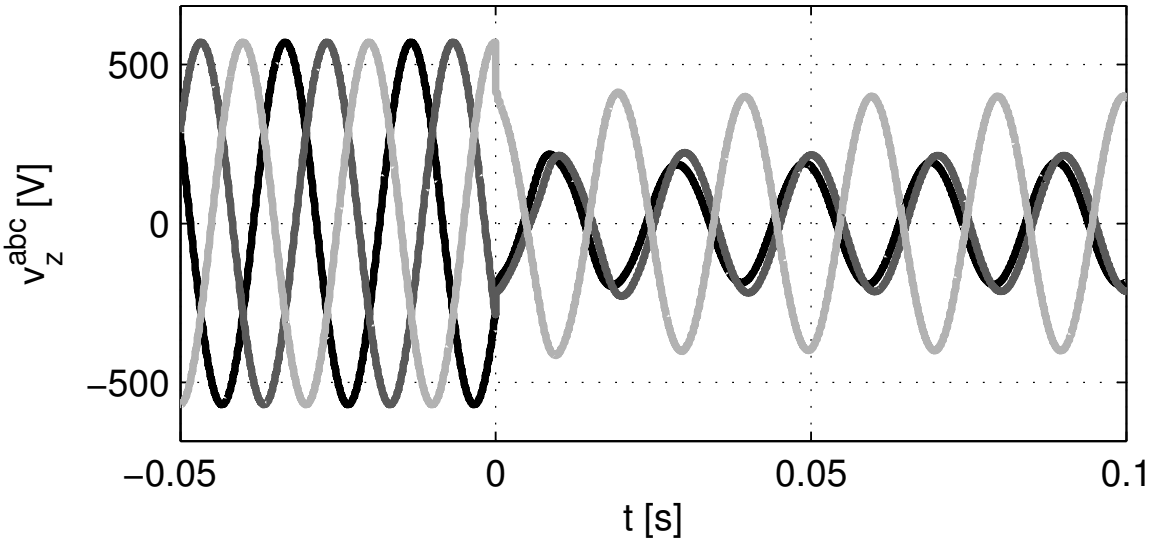

Fig. 3. Voltage at the PCC of the converter.

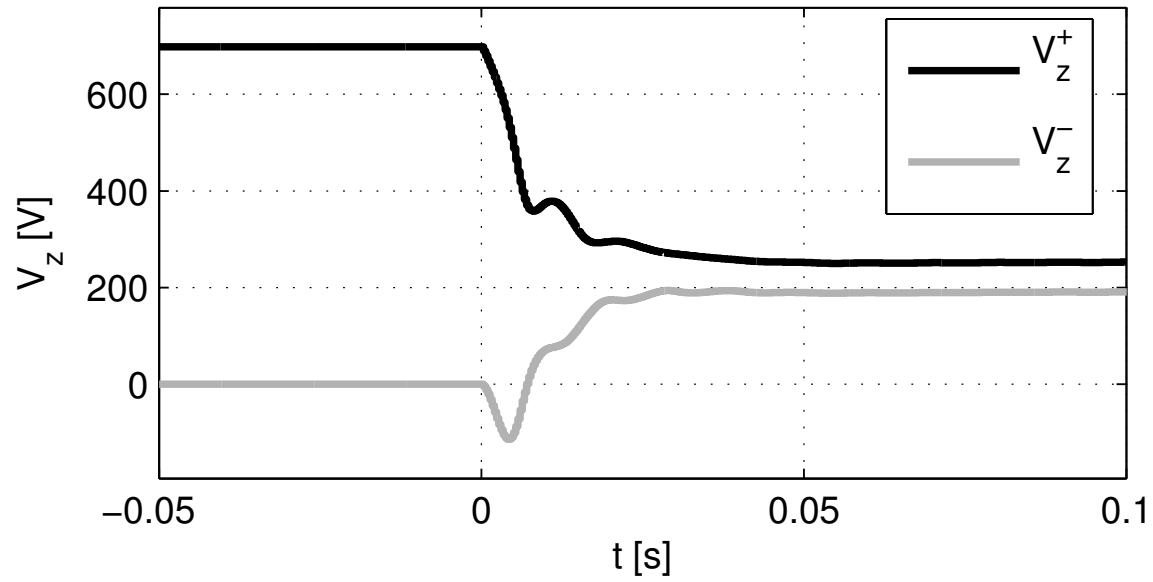

Fig. 4. Amplitude of the positive and negative sequence of the voltage at the PCC measured by the PLL.

The controller used in the simulation model uses the double synchronous reference frame (DSRF) current controller described in [11] and a PLL for unbalanced voltages described in [20]. The performance specifications for both parts of the controller can be found in Table I.

Figure 5 shows the evolution of the voltage during the sag. Notice that the initial transient is the same for all the methods as expected but the steady state differs. Methods I and III produce a significant steady state ripple, the reason for that is that method I does not use negative sequence and method III does not compensate the difference between the power on the grid connection point and the power on the inverter terminals. This can further be confirmed by plotting P_l and P_z (Figure 6). Notice that method III allows to suppress the ripple in P_z but causes an important ripple in P_l which makes the DC bus voltage to have a larger oscillation than method I.

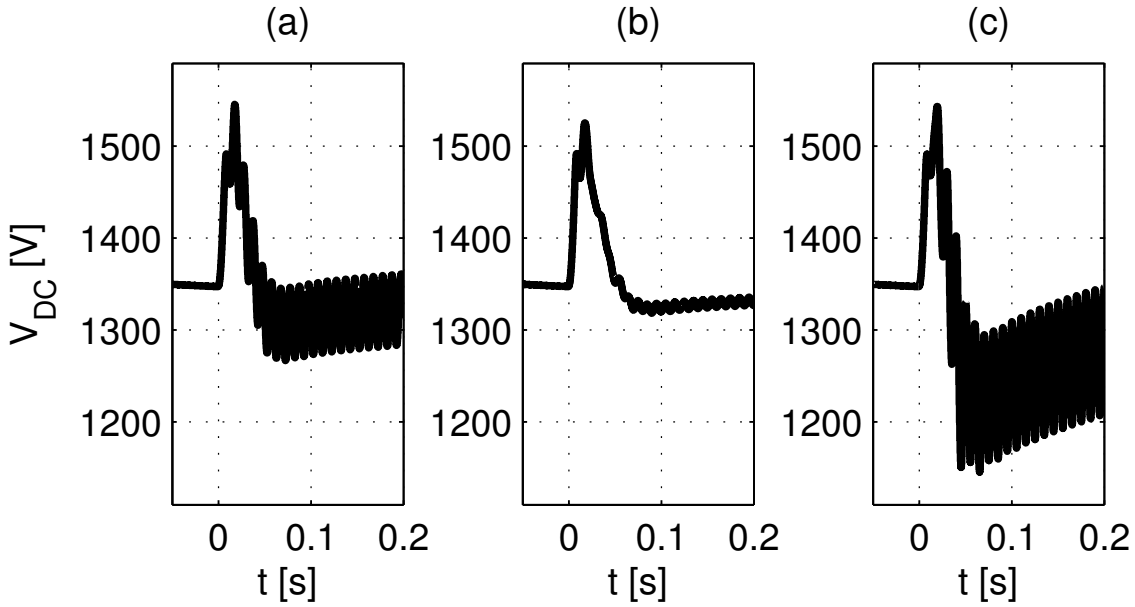

Fig. 5. Comparison of the evolution of the DC bus voltage using I (a), II (b) and III (c) current reference calculation methods.

The evolution of the current is shown in Figure 7. Note that all methods require an increase of the current due to the reduction of the voltage and as noted before methods II and III require more current than I even though the oscillation in III is larger than in I.

VI. Experimental testing of the proposed reference calculation scheme

In order to further verify the theoretical results, a test of the analyzed current reference calculation schemes is performed on an experimental platform. The test platform consists of two CDM2480 [21] low power voltage source three phase inverters fed by two independent 24V DC buses and connected by the AC side through a three phase inductor ($r = 0.1\ \Omega$, $L = 4.9$ mH). One of the inverters, referred as the generator grid side inverter, is used to emulate the grid side inverter of a grid connected power source and inject power from its DC bus to the other inverter, referred as the grid emulator, used to emulate the behaviour of the grid. A picture and a diagram of the

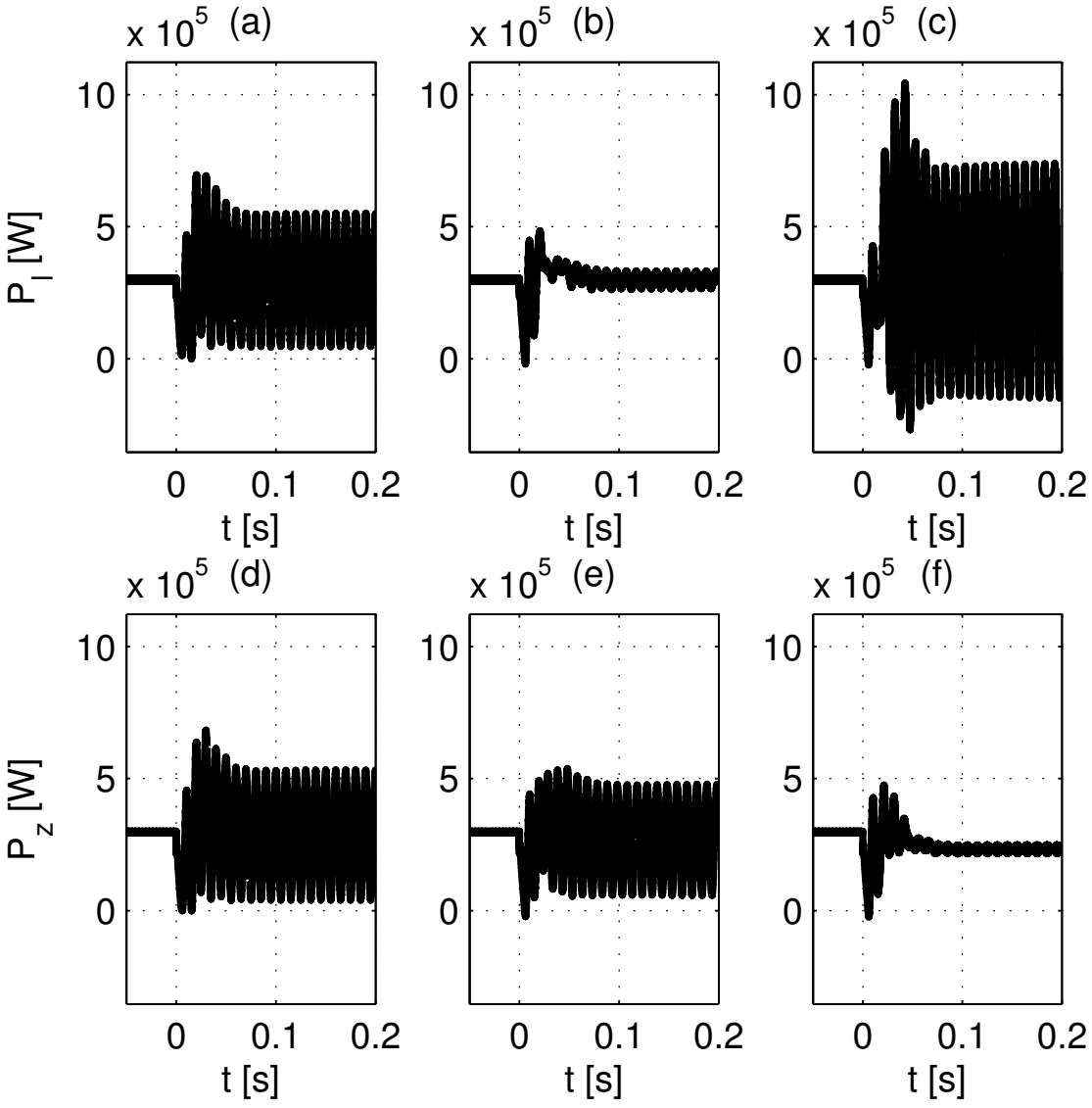

Fig. 6. Comparison of the evolution of the converter output power measured on the inverter versus the power measured on the PCC using I (a,d), II (b,e) and III (c,f) current reference calculation methods.

differents parts of the experimental setup can be seen in Figure 8. The voltage of the terminals of the generator side inverter and the grid emulator and the current flowing through the inductors are measured and recorded using a data adquisition device.

Each inverter is controlled by a TMS320F2812 eZdsp^{TM} control board which have been programmed for the test. The grid emulator inverter is programmed to apply three phase voltage waveforms on its AC side corresponding to those of the two phase fault used in the simulations in the previous section whilst the current flowing thorugh the generator side inverter is controlled using a DSRF current controller as in the simulated scenario of the previous

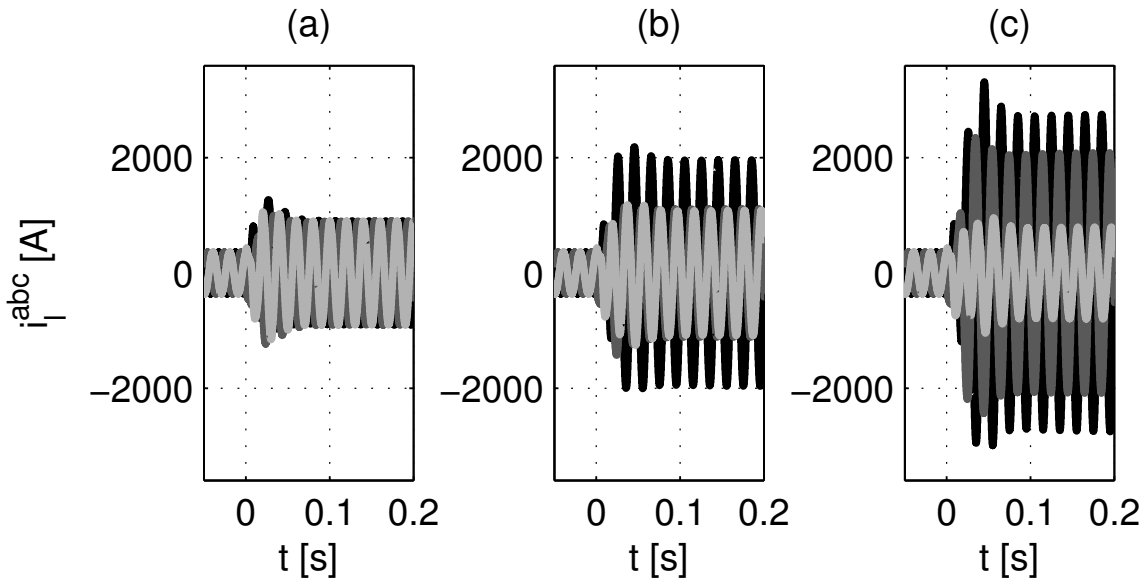

Fig. 7. Comparison of the output current of the converter using I (a), II (b) and III (c) current reference calculation methods.

section.

Three different tests of the response of the system under the same unbalanced voltage sag are performed on the experimental platform using a different current reference calculation method each time. The evolution of the grid voltage, the current and the active power flowing through the converter and the active power injected to the grid for each scheme can be seen in Figures 9, 10 and 11. It can be seen that the voltage sag requires an increase of the current to keep the same average power output from the converter in any case. In the case of method I, which only injects positive sequence current, the increase is smaller and symmetrical for each phase, whereas methods II and III require asymmetrical currents which are higher in, at least, one of the phases. Regarding the power ripple, method I produces an important ripple both in the power injected to the grid and the converter output. Method III is able to compensate the ripple in the power injected to the grid but produces a higher ripple in the converter output power. By compensating the effect of the inductor impedance, method II is able to suppress that ripple but then produces a ripple in the power injected to the grid.

VII. Conclusions

The injection of negative sequence currents have been shown to allow to suppress the oscillation on the DC bus voltage due to the oscillation of the power injected to the grid during a unbalanced voltage sag. However, compared to the standard method of injecting only positive sequence current, this method have been found to require larger currents to maintain the same level of average active power. For deep voltage sags, this may lead to even higher oscillations of the DC bus voltage if the effect of the AC filter impedance on the converter power output is not properly compensated and a method has been proposed to do it. Also, a special condition has been identified which

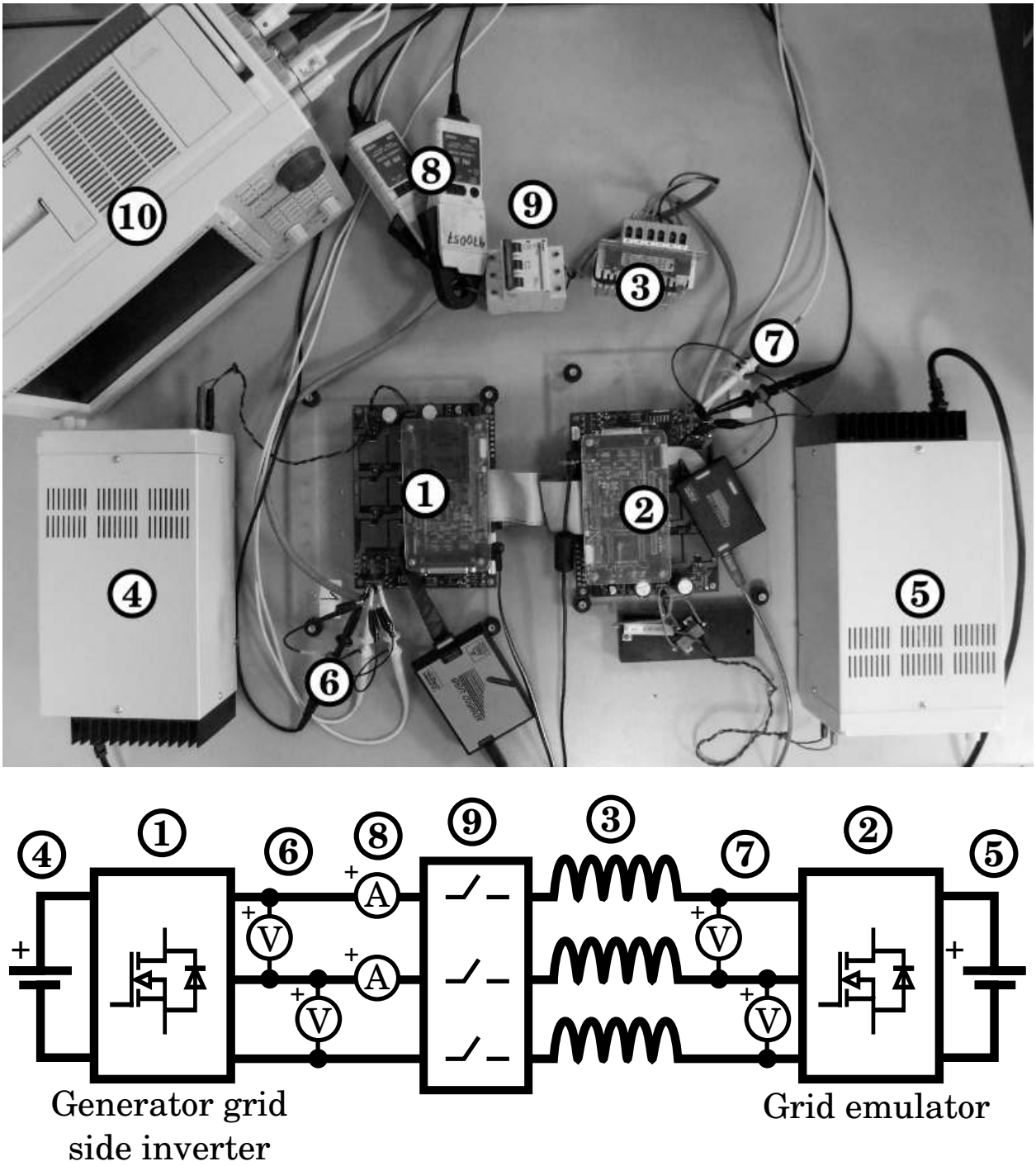

Fig. 8. Picture and schematics of the experimental setup. (1) generator grid-side inverter, (2) grid emulator, (3) converter inductances, (4) generator-side DC power source, (5) grid emulator DC power source and load, (6) generator grid-side inverter voltage v_l^{abc} measurement, (7) grid emulator voltage v_z^{abc} measurement, (8) generator grid-side output current i_l^{abc} measurement, (9) grid connection switch, (10) data adquisition device.

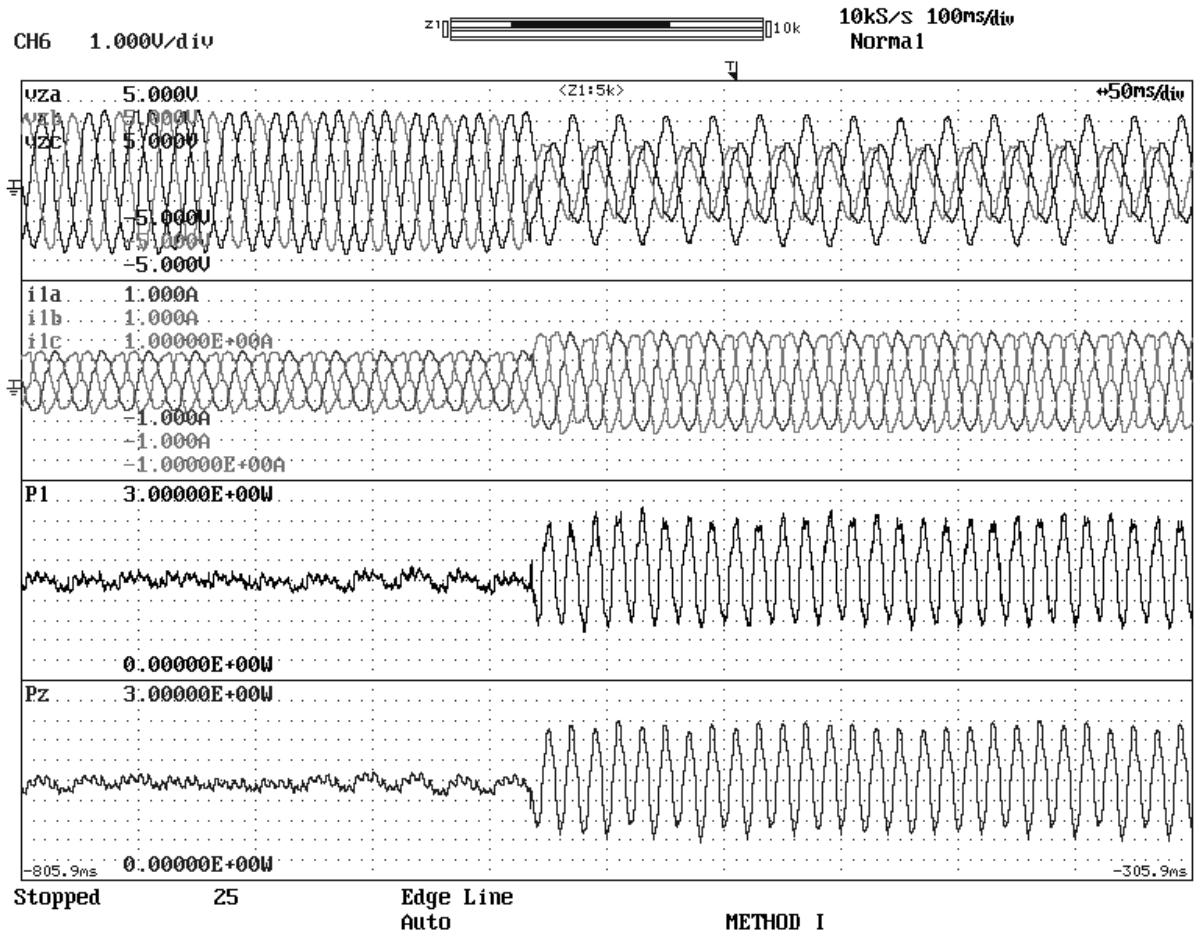

Fig. 9. Experimental results for method I. From top to bottom: v_z^{abc},i_l^{abc},P_l and P_z.

makes it impossible to control the oscillating terms of the active power and a solution for the calculation of the current references in that case has been proposed.

REFERENCES

[1] C. Sao and P. Lehn, "Control and power management of converter fed microgrids," *Power Systems, IEEE Transactions on*, vol. 23, no. 3, pp. 1088 –1098, 2008. 1

[2] O. Gomis-Bellmunt, J. Liang, J. Ekanayake, R. King, and N. Jenkins, "Topologies of multiterminal hvdc-vsc transmission for large offshore wind farms," *Electric Power Systems Research*, vol. 81, pp. 271–281, 2011. 1

[3] V. Blasko and V. Kaura, "A new mathematical model and control of a three-phase ac-dc voltage source converter," *Power Electronics, IEEE Transactions on*, vol. 12, no. 1, pp. 116 –123, Jan. 1997. 1

[4] S. Buso, *Digital Control in Power Electronics (Synthesis Lectures on Power Electronics)*. Morgan and Claypool Publishers, 2006. 1, 3

[5] M. H. Bollen, *Understanding Power Quality Problems: Voltage Sags and Interruptions*. Wiley-IEEE Press, 1999. 2

[6] J. Morren and S. de Haan, "Ridethrough of wind turbines with doubly-fed induction generator during a voltage dip," *Energy Conversion, IEEE Transactions on*, vol. 20, no. 2, pp. 435 – 441, 2005. 2

[7] C. Feltes, H. Wrede, F. Koch, and I. Erlich, "Enhanced fault ride-through method for wind farms connected to the grid through vsc-based hvdc transmission," *Power Systems, IEEE Transactions on*, vol. 24, no. 3, pp. 1537 –1546, 2009. 2

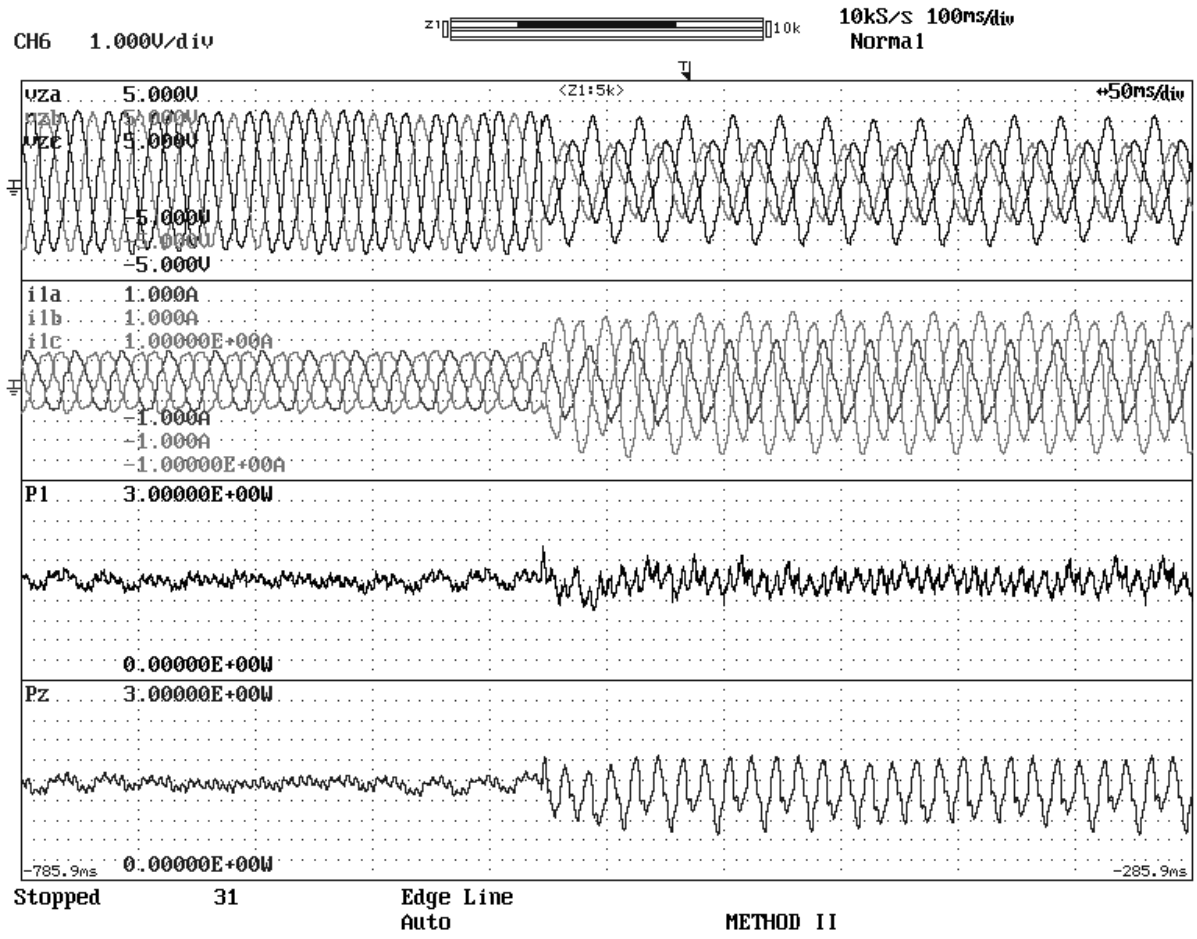

Fig. 10. Experimental results for method II. From top to bottom: v_z^{abc},i_l^{abc},P_l and P_z.

[8] P. Rioual, H. Pouliquen, and J.-P. Louis, "Regulation of a pwm rectifier in the unbalanced network state using a generalized model," *IEEE Transactions on Power Electronics*, vol. 11, no. 3, pp. 495–502, May 1996. 2

[9] H. Song and K. Nam, "Dual current control scheme for PWM converter under unbalanced input voltage conditions," *IEEE Transactions on Industrial Electronics*, vol. 46, no. 5, pp. 953–959, Oct. 1999. 2

[10] L. Xu, "Coordinated control of dfig's rotor and grid side converters during network unbalance," *IEEE Transactions on Power Electronics*, vol. 23, pp. 1041–1049, 2008. 2

[11] O. Gomis-Bellmunt, A. Junyent-Ferre, A. Sumper, and J. Bergas-Jané, "Ride-through control of a doubly fed induction generator under unbalanced voltage sags," *IEEE Transactions on Energy Conversion*, vol. 23, pp. 1036–1045, 2008. 2, 8, 13

[12] S. Alepuz, S. Busquets-Monge, J. Bordonau, J. Martinez-Velasco, C. C.A. Silva, J. Pontt, and J. Rodriguez, "Control strategies based on symmetrical components for grid-connected converters under voltage dips," *IEEE Transactions on Industrial Electronics*, vol. 56, pp. 2162–2173, 2009. 2

[13] Y. Zhou, P. Bauer, J. Ferreira, and J. Pierik, "Operation of grid connected dfig under unbalanced grid voltage condition," *IEEE Transactions on Energy Conversion*, vol. 24, pp. 240–246, 2009. 2

[14] J. Hu, Y. He, L. Xu, and B. Williams, "Improved control of dfig systems during network unbalance using pir current regulators," *IEEE Transactions on Industrial Electronics*, vol. 56, pp. 439–451, 2009. 2

[15] Z. Li, Y. Li, P. Wang, H. Zhu, C. Liu, and W. Xu, "Control of three-phase boost-type pwm rectifier in stationary frame under unbalanced input voltage," *Power Electronics, IEEE Transactions on*, vol. 25, no. 10, pp. 2521 –2530, oct. 2010. 2

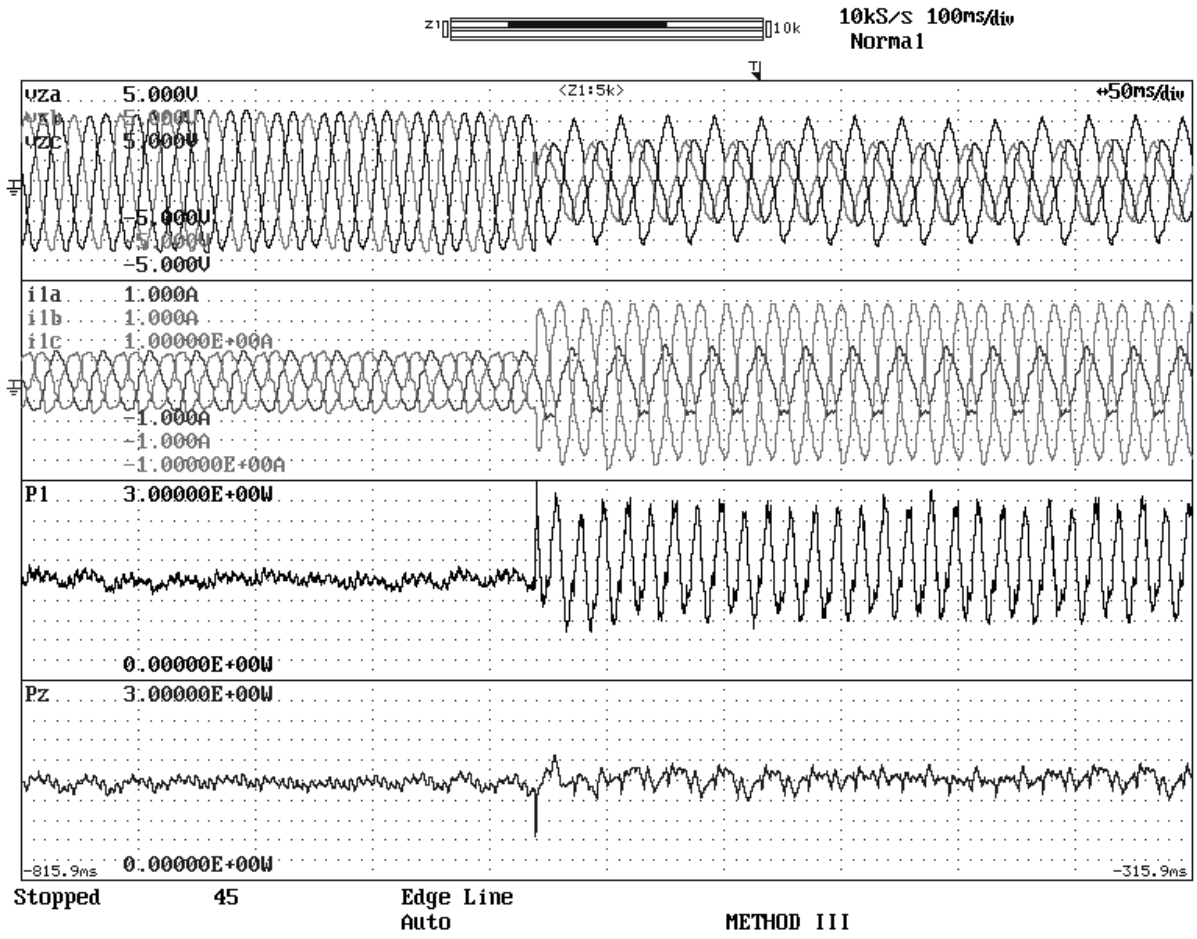

Fig. 11. Experimental results for method III. From top to bottom: v_z^{abc},i_l^{abc},P_l and P_z.

[16] C.-M. Ong, *Dynamic Simulations of Electric Machinery: Using MATLAB/SIMULINK*. Prentice Hall, 1997. 4

[17] C. L. Fortescue, "Method of symmetrical co-ordinates applied to the solution of polyphase networks," *American Institute of Electrical Engineers, Transactions of the*, vol. XXXVII, no. 2, pp. 1027 –1140, 1918. 4, 6

[18] H. Akagi, E. H. Watanabe, and M. Aredes, *Instantaneous Power Theory and Applications to Power Conditioning (IEEE Press Series on Power Engineering)*. Wiley-IEEE Press, 2007. 5

[19] A. Junyent-Ferré, O. Gomis-Bellmunt, A. Sumper, M. Sala, and M. Mata, "Modeling and control of the doubly fed induction generator wind turbine," *Simulation Modelling Practice and Theory*, vol. 18, no. 9, pp. 1365 – 1381, 2010. 11

[20] M. Karimi-Ghartemani and H. Karimi, "Processing of symmetrical components in time-domain," *IEEE Transactions on Power Systems*, vol. 22, pp. 572–579, 2007. 13

[21] D. Montesinos, S. Galceran, A. Sudria, and O. Gomis, "A laboratory test bed for pm brushless motor control," in *Power Electronics and Applications, 2005 European Conference on*, 0-0 2005, pp. 6 pp. –P.6. 13